

Operational earthquake loss forecasting: a retrospective analysis of some recent Italian seismic sequences

Eugenio Chioccarelli¹ and Iunio Iervolino^{2,*}

¹*Analisi e Monitoraggio dei Rischi Ambientali (AMRA) scarl, Naples, Italy.*

eugenio.chioccarelli@amrcenter.com

²*Dipartimento di Strutture per l'Ingegneria e l'Architettura, Università degli Studi di Napoli Federico II, Naples, Italy.*

iunio.iervolino@unina.it

Abstract

Operational earthquake forecasting (OEF) relies on real-time monitoring of seismic activity in an area of interest to provide constant (e.g., daily) updates of the expected number of events exceeding a certain magnitude threshold in a given time window (e.g., one week). It has been demonstrated that the rates from OEF can be used to estimate expected values of the seismic losses in the same time interval OEF refers to. This is a procedure recently defined as *operational earthquake loss forecasting* (OELF), which may be the basis for rational short-term seismic risk assessment and management.

In Italy, an experimental OELF system, named MANTIS-K, is currently under testing. It is based on weekly rates of earthquakes exceeding magnitude (M) 4, which are updated once a day or right after the occurrence in the country of an M 3.5+ earthquake. It also relies on large-scale structural vulnerability and exposure data, which serve to the system to provide continuously the expected number of: (i) collapsed buildings, (ii) displaced residents, and (iii) casualties.

While the probabilistic basis of MANTIS-K was described in previous work, in this study OELF is critically discussed with respect to three recent Italian seismic sequences. The aim is threefold: (i) illustrating all the features of the OELF system in place; (ii) providing insights useful to evaluate whether if it would have been a useful additional tool for short-term management; (iii) recognizing common features, if any, among the losses computed for different sequences.

Keywords: seismic risk management; seismic loss.

* Corresponding author. Dipartimento di Strutture per l'Ingegneria e l'Architettura, Università degli studi di Napoli Federico II, via Claudio 21, 80125, Naples, Italy. Tel: +39 081 7683488; Fax: +39 081 7685921.

26 **1. Introduction**

27 The seismological community is investing in development and application of stochastic models for forecasting
28 the space-time distribution of earthquakes conditional on the seismic history at the time of the probabilistic
29 evaluation: e.g., epidemic type aftershock sequence or ETAS (Ogata, 1988 and 1998) and short-term
30 earthquake probability or STEP (Gerstenberger et al., 2005) models. The common assumption is that each
31 event of a seismic sequence can trigger new events causing an alteration of the seismicity in the area where it
32 strikes; i.e., no physical differences are assumed among foreshocks, mainshocks and aftershocks (Jordan et al.,
33 2011). Coupling this kind of models with real-time data acquired from monitoring seismic networks, the
34 resulting systems can constantly provide *operational earthquake forecasting* (OEF). In Italy, an OEF prototype
35 (OEF-Italy) of the national institute of geophysics and volcanology (INGV) is currently under testing in order
36 to evaluate whether it is suitable to provide information about the short-term seismic hazard to the Italian civil
37 protection system (Marzocchi et al., 2014).

38 In fact, the output of OEF can be useful for risk management if the rates of events above a magnitude
39 threshold of interest may be used as an input for probabilistic assessment of seismic losses (e.g., Marzocchi et
40 al., 2015). A procedure to do so, that is converting outputs of OEF into loss-related measures in a
41 probabilistically consistent manner, has been recently developed and defined as *operational earthquake loss*
42 *forecasting* (OELF; Iervolino et al., 2015a). In fact, a prototype system for OELF, called MANTIS-K, is also
43 currently under experimentation in Italy. It starts from the weekly earthquake rates continuously provided (i.e.,
44 daily or after an event 3.5+ in magnitude) by OEF-Italy, and combines them with exposure data (at the scale
45 of municipality) and models about seismic vulnerability of the building stock, to compute weekly expected
46 values of seismic loss metrics after each OEF rates release.

47 Validation of expected losses requires a large amount of observed data, certainly unavailable in the
48 case of MANTIS-K at this point. In fact, validation is out of the scope of this paper; however, referring to past
49 seismic sequences, a critical analysis of the results provided by the system, during seismic sequences that
50 raised risk management issues, may be useful. It may help understanding whether OELF, in the analysed cases,
51 would have been a useful additional instrument for short-term management. Moreover, the retrospective
52 analyses herein presented allow describing the type of information provided by MANTIS-K and recognizing

53 common features, if any, among the losses forecasted during three sequences, which are quite different from
54 the seismological perspective.

55 As it regards the structure of the paper, even if details can be found in Iervolino et al. (2015a), the
56 main equations and implemented models of MANTIS-K are summarised first. Subsequently, the three selected
57 Italian seismic sequences are presented. They are those with the largest magnitude events occurred in Italy
58 from 2004 to 2014 (excluding those offshore) and are named as *L'Aquila* (2009), *Emilia* (2012) and
59 *Garfagnana* (2013). For each sequence, a general description is provided and the evolution of the earthquake
60 rates forecasted by OEF-Italy, for each day in a selected period, is presented. Then, the daily-updated loss
61 indices, forecasted by MANTIS-K in the area of the sequence, are shown; i.e., the expected values of fatalities,
62 unusable buildings, and displaced residents, in the time-horizon of one week after each OEF data release.
63 These indices are computed referring to four groups of municipalities characterised by increasing distance
64 from the epicentre of the mainshock of the sequence. The work is concluded by a comparison of the OELF
65 results among the sequences and a discussion with respect to the observed losses.

66 **2. MANTIS-K system for operational earthquake loss forecasting in Italy**

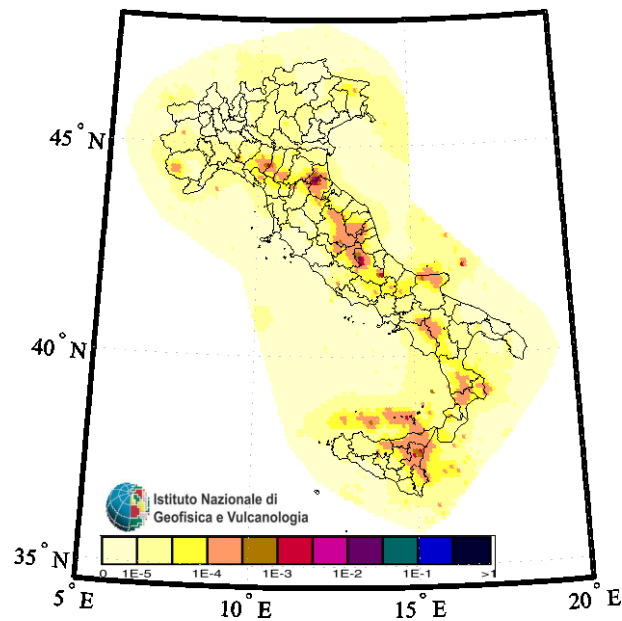
67 If data from a seismic sensor network monitoring a given region are available at each time instant t , that is, the
68 seismic history, $H(t)$, is known, OEF models provide an estimation of future seismicity. More specifically,
69 according to OEF, the territory is divided into elementary areas which are identified by pairs of coordinates
70 $\{x, y\}$. Each area is considered as a point-like seismic source to which OEF assigns an expected number of
71 generated earthquakes above a magnitude of interest per unit-time; i.e., the seismic rate. Such a rate,
72 $\lambda[t, x, y | H(t)]$, depending on the recorded seismic history, varies with t .

73 In Italy, an OEF system is operating (Marzocchi et al., 2014). It is based on the country-wide seismic
74 network of INGV and provides, for a grid of about 9000 point-like seismic sources spaced of about 0.1° and
75 covering the whole Italian territory and some sea, the seismic rates updated at least once a day and every time
76 an earthquake of local magnitude (M_L) equal or larger than 3.5 occurs. These rates are the forecasted mean
77 number of M_L 4.0+ events produced by the point source in a time-horizon of one week. The probability density
78 function of the magnitude of the events, $f_M(m)$ in the following, is assumed to be derived from a Gutenberg-

79 Richter-type relationship (Gutenberg and Richter, 1944), with unbounded maximum magnitude and b -value
80 equal to one. This is common to all the point sources, that is, differences among the sources derive only from
81 the seismic rates.

82 Although a prototypal version of the system has started working on the 7th of April 2009 (Marzocchi
83 and Lombardi, 2009), the complete Italian seismic catalogue from April 2005 to June 2014 has been analysed
84 offline by the OEF-Italy system and the seismic rates for the whole grid of point sources have been computed
85 at 00:00 of each day. A database collecting all the results for the analysed period (about 3300 days) has been
86 provided to the authors (Warner Marzocchi, personal communication, July, 2014) and has been used for the
87 analyses presented in the following.

88 An example of the seismic rates provided by OEF-Italy system is reported in Figure 1 for illustrative
89 purpose. The picture, arbitrarily, refers to the OEF-Italy results computed at 00:00 of the 6th of April 2009.



90
91 Figure 1. Map of expected number of $M_L \geq 4$ events in the week following 00:00 of 06/04/09, estimated through OEF-
92 Italy.

93 In Iervolino et al. (2015a), it has been demonstrated that, starting from the rates resulting from the OEF-Italy
94 system, it is possible to derive indices of seismic losses via a probabilistically sound procedure. The latter
95 involves models used in the classical probabilistic seismic hazard analysis (PSHA; e.g. McGuire, 2004), and
96 is consistent with the performance-based earthquake engineering (Cornell and Krawinkler, 2000) framework.
97 While the interested reader should refer to the given reference for details, such a procedure for OELF is

98 summarised here for the sake of readability of the results of the study. In fact, the equation and the models
99 required are recalled as well as the data and models used for Italy.

100 **2.1 Hazard (shaking intensity)**

101 Starting from the weekly seismic rates from OEF-Italy described above, $\lambda[t, x, y | H(t)]$, associated to each
102 point-like seismic source in Italy, MANTIS-K associates probabilities of shaking intensity in terms of
103 macroseismic (MS) intensity. This is because the vulnerability models considered (to follow) are function of
104 MS .

105 Prediction equations allow estimating the probability of a specific MS intensity at the generic site,
106 identified by the couple of coordinates $\{w, z\}$, conditional on the occurrence of an earthquake of known
107 magnitude, M , at a given point-like seismic source; i.e., $P[MS = ms | m, R(x, y, w, z)]$, being $R(x, y, w, z)$
108 the source-to-site distance. The chosen prediction equation for macroseismic intensity is that of Pasolini et al.
109 (2008) that identified intensity as defined by the Mercalli-Cancani-Sieberg (MCS) scale (Sieberg, 1931). The
110 model applies to the [0 km, 220 km] interval of the distance,[†] and between 5 and 12 of intensity.

111 **2.2 Vulnerability**

112 Structural vulnerability is accounted for in MANTIS-K via a damage probability matrix (DPM) that, according
113 to the definition of Whitman et al. (1973) and Braga et al. (1982), provides the probability of observing a
114 damage state (ds) to a building of a given structural typology (k), given a value of intensity, ms , at the site;
115 i.e., $P[DS^{(k)} = ds | ms]$. The DPM considered is based on Italian observational data (Zuccaro and Cacace,
116 2009; Iervolino et al., 2014a). It accounts for four different vulnerability classes in which the Italian building
117 stock is divided, from A to D (the same as indicated in European Macroseismic Scale EMS 98), and six damage
118 levels (D0 – no damage, D1 – slight damage, D2 – moderate damage, D3 – heavy damage, D4 – very heavy
119 damage, D5 collapse).

[†] However, in the loss assessment, contributions from sources with epicentral distance larger than 150 km are neglected.

120 Another model used is, for the k -th structural typology and conditional on damage state, the probability
 121 for an occupant to suffer casualties, $P[Cas^{(k)}|ds]$. Casualty probabilities, conditional on structural damage
 122 and vulnerability class, are those of Zuccaro and Cacace (2011). Such a model refers to two types of casualties;
 123 i.e., (i) fatalities and (ii) injuries (someone requiring hospital treatment is considered as injured).

124 2.3 Exposure

125 In Italy, the elementary units for which dwelling building exposure data are made publicly available from the
 126 population census are municipalities. For this reason, all computations performed by MANTIS-K refer to the
 127 municipality level and to dwelling buildings only: the centroid of each municipality area is the $\{w, z\}$ point
 128 used for computing the source-to-site distance and in which all exposed assets in the municipality are supposed
 129 to be concentrated. For each municipality, exposure in terms of building is the number of buildings of k -th
 130 typology, $N_b^{(k)}$. The number of residents living in the k -th building typology, $N_p^{(k)}$, is a measure of exposure
 131 in terms of residents. Both kinds of data are derived from the National census of 2001 (Zuccaro et al., 2012).
 132 Note that these exposure measures depend on the municipality, that is on $\{w, z\}$; however, the coordinates are
 133 dropped for simplicity in the symbols.

134 2.4 Losses

135 Assuming that the stochastic process of events causing damage to the building at the site is approximated, in
 136 the short time interval (Δt) , by a homogeneous Poisson process, the expected number of casualties (fatalities
 137 or injuries) in the considered $\{w, z\}$ municipality, $E[N_{Cas,(t,t+\Delta t)}|H(t)]$, can be computed via equation (1).
 138 According to Zuccaro et al. (2012), casualty and injury assessments are carried out considering that 65% of
 139 the total population is exposed at the time of occurrence of the earthquake, which justifies 0.65 in the equation.

$$\begin{aligned}
 & E[N_{Cas,(t,t+\Delta t)}|H(t)] \approx \Delta t \cdot \sum_k 0.65 \cdot N_p^{(k)} \cdot \iint_{x,y} \lambda[t, x, y|H(t)] \cdot \sum_{ds} P[Cas^{(k)}|ds] \cdot \\
 & \cdot \sum_{ms} P[DS^{(k)} = ds|ms] \cdot \int_m P[MS = ms|m, R(x, y, w, z)] \cdot f_M(m) \cdot dm \cdot dx \cdot dy
 \end{aligned} \tag{1}$$

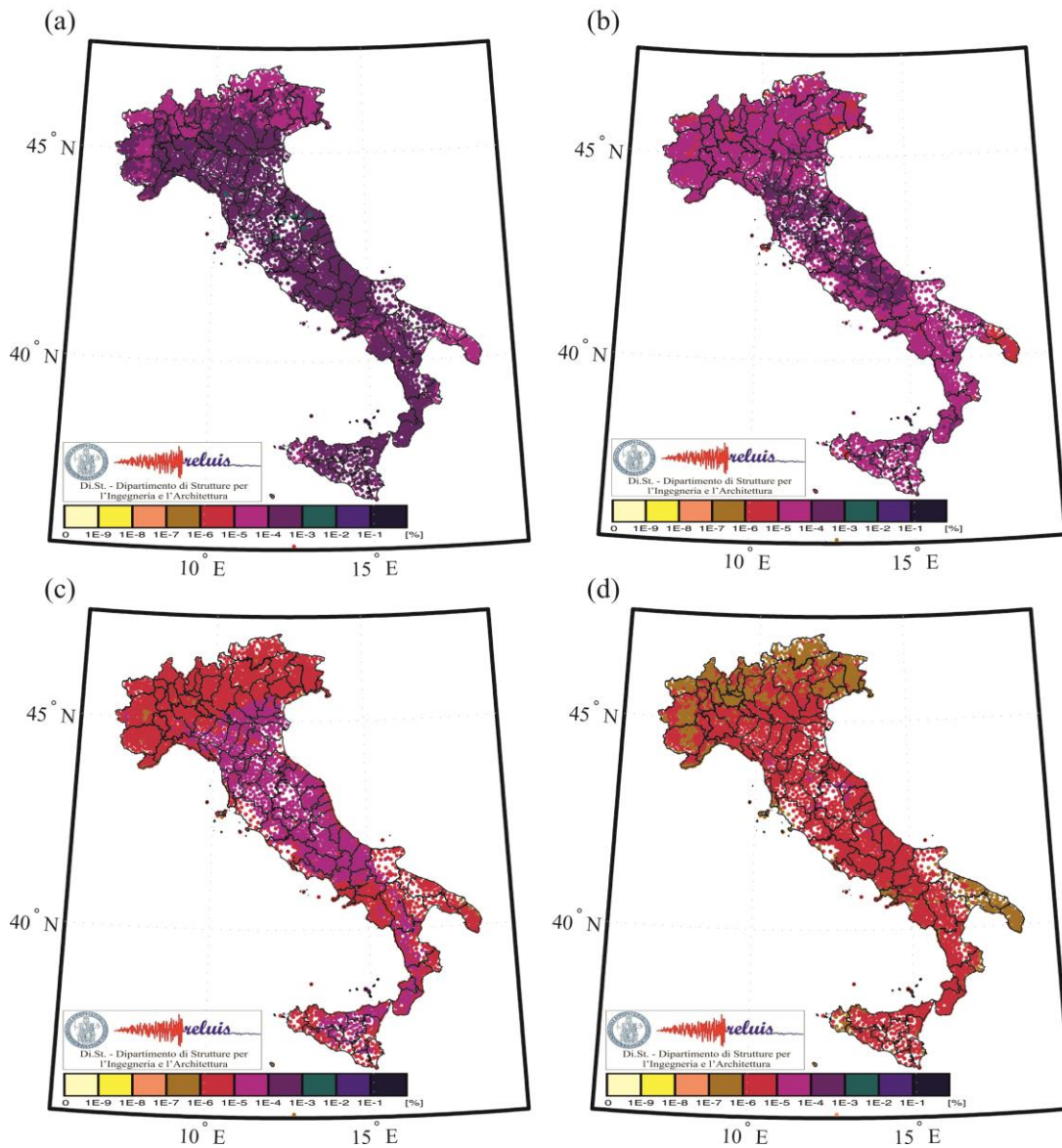
141 Zuccaro and Cacace (2011) also provide the probability of a building to be unusable for a given damage state,
 142 $P[Unus|ds]$. Such a probability, which does not depend on the structural typology, is 1 for damage state D4
 143 and D5, whereas it is 0.5 for buildings in D3, and it is 0 for lower damage levels. Thus, the expected number
 144 of unusable buildings in one time unit, $E[N_{Unus,(t,t+\Delta t)}|H(t)]$, can be computed via equation (2).

$$\begin{aligned}
 E[N_{Unus,(t,t+\Delta t)}|H(t)] &\approx \Delta t \cdot \sum_k N_b^{(k)} \cdot \iint_{x,y} \lambda[t,x,y|H(t)] \cdot \sum_{ds} P[Unus|ds] \cdot \\
 145 &\cdot \sum_{ms} P[DS^{(k)} = ds|ms] \cdot \int_m P[MS = ms|m, R(x,y,w,z)] \cdot f_M(m) \cdot dm \cdot dx \cdot dy
 \end{aligned} \tag{2}$$

146 Replacing the number of buildings, $N_b^{(k)}$, with the number of residents, $N_p^{(k)}$, the expected number of displaced
 147 residents may also be computed. Indeed, all the residents living in an unusable building are considered as
 148 shelter-seeking.

149 To give a sense of the results MANTIS-K provides with these models and data, Figure 2 shows, for
 150 each municipality, the expected values of: (a) unusable and (b) collapsed buildings (values are per 100
 151 buildings), and the expected value of (c) injuries and (d) fatalities (both per 100 residents), on the basis of the
 152 OEF-Italy data of Figure 1. Indeed, these results are the losses forecasted for the week after the OEF rates'
 153 release (00:00 on 06/04/09), and the same weekly horizon will be maintained for all results shown in the
 154 following sections of the paper.

155 The previous equations may be considered as site-specific risk measures as they apply to
 156 municipalities; however, they can be summed over an area of interest to compute total expected losses.



157

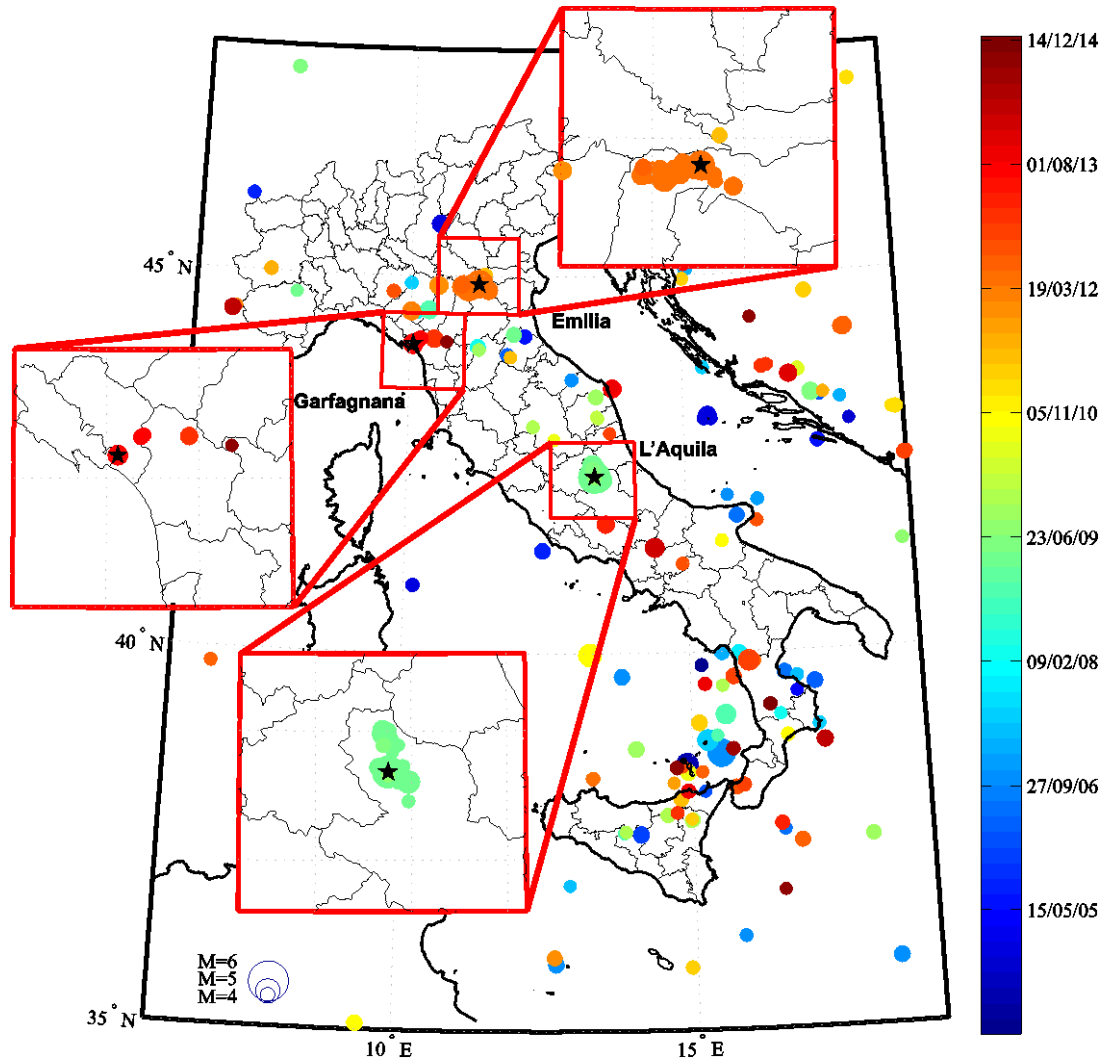
158 Figure 2. Illustrative example of MANTIS-K outputs: maps of the expected values of (a) unusable and (b) collapsed per
 159 100 buildings, and the expected values of (c) injuries and (d) fatalities per 100 municipality residents. These results are
 160 computed using the OEF-Italy data of Figure 1 as the input. Therefore they refer to the week after 00:00 of 06/04/09.

161 **3. Considered Italian seismic sequences**

162 From 2004 to 2014 more than two-hundreds M 4.0+ events occurred in Italy (i.e., in a geographic area
 163 identified by 35.0-48.0 °N latitude and 6.0-19.0 °E longitude).[‡] Epicentral locations of these events are plotted
 164 in Figure 3; the size of each circle is proportional to the magnitude and the colour relates to the date of the
 165 event. Earthquakes with the largest magnitude identify three seismic sequences named *L'Aquila*, *Emilia* and

[‡] Data from ISIDE, <http://iside.rm.ingv.it/>, last accessed 20/07/15. Because ISIDE does not provide measures is a unique magnitude scale for all the events, M without subscripts is used where necessary.

166 *Garfagnana*, due to the areas where they occurred (identified in the same figure). For each sequence, the
 167 epicentre of the largest magnitude event (i.e., the mainshock) is indicated as a star; these points are referred to
 168 as the centres of the corresponding seismic sequence hereafter.



169
 170 Figure 3. Epicentres of $M \geq 4$ seismic events occurred from 01/01/04 to 31/12/14 and geographic areas considered for the
 171 three sequences analysed.

172 L'Aquila and Emilia sequences were characterised by significant losses in terms of structural damages and
 173 fatalities. The same did not happen in Garfagnana; however, during this sequence, the Italian civil protection
 174 system was in state of alert for the possible occurrence of damaging events, after a M_w 5.1 earthquake. For
 175 this reason, the Garfagnana seismic sequence has been considered in the context of this study.

176 The retrospective analysis of each sequence consisted of the computation of the expected losses for the
 177 week following each day for which forecasted seismicity was available by OEF-Italy. In the following, each
 178 seismic sequence is presented first and the rates computed by OEF-Italy are reported as function of time and

179 summed up over the point-like sources within 30 km from the centre of the sequence, to get a sense of the
 180 forecasted seismicity in the area. Then, the evolution of some indices of seismic losses from MANTIS-K are
 181 reported and compared among sequences. Finally, a discussion with respect to the observed consequences is
 182 given.

183 The considered risk metrics, computed by MANTIS-K for each municipality, are the expected values in
 184 one week of: (i) fatalities and (ii) displaced residents, (iii) unusable and (iv) collapsed dwelling buildings.
 185 Results are reported as the expected value of total loss within four areas identified by the maximum distance
 186 (10 km, 30 km, 50 km and 70 km) from the epicentre of the mainshock;[§] see Figure 4b. For the sake of
 187 presentation, arbitrarily, a time window spanning three months before and one year after the mainshock is
 188 considered.

189 3.1 L'Aquila 2009

226 The main event of L'Aquila sequence, moment magnitude (M_w) 6.1, struck on the 6th of April 2009; it
 227 produced a maximum observed peak ground acceleration (PGA) equal to 644 cm/s^2 (e.g., Chioccarelli et al.,
 228 2009; Dolce and Di Bucci, 2015). In the area identified by $41.8\text{-}42.8^\circ \text{N}$ latitude and $12.6\text{-}14.1^\circ \text{E}$ longitude
 229 (red square in Figure 1), a single $M 4+$ event occurred before the mainshock since the 1st of January 2009, that
 230 is, the $M_w 4.0$ on the 30th of March 2009. In the same area and period, there were 29 $M 2.5+$ events and 10 M
 231 $3.0+$. On the other hand, the aftershock sequence was characterised by 8 $M 4.5+$ earthquakes, reported in Table
 232 1 (along with mainshock data), and more than 300 events $M 2.5+$ in the 24 hours after the mainshock.

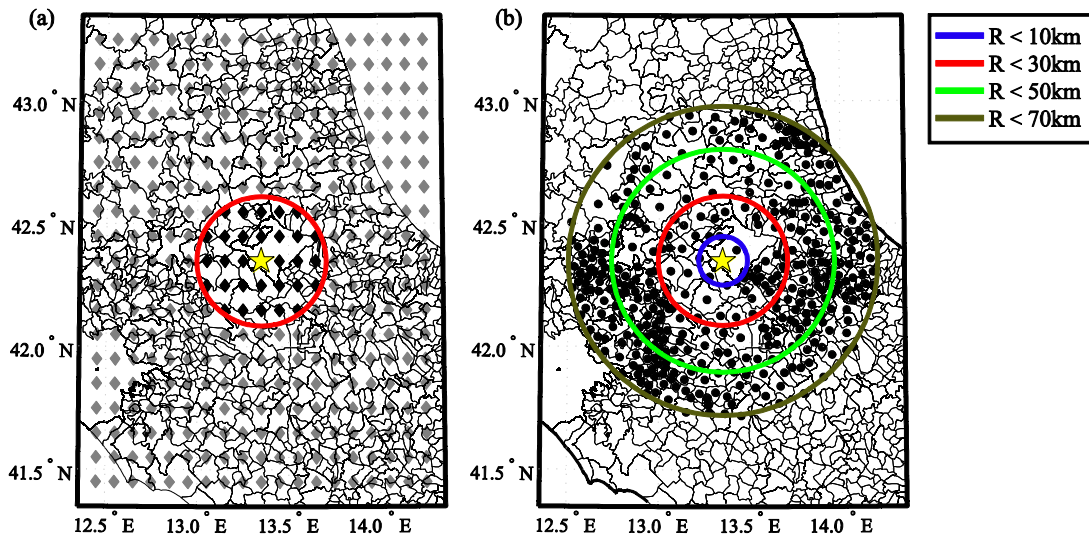
233 Table 1. $M 4.5+$ aftershocks in a geographic area within latitude $41.8^\circ\text{-}42.8^\circ$ and longitude $12.6^\circ\text{-}14.1^\circ$. Reported
 234 information are event date and time, hypocentre latitude, longitude and depth, event magnitude. Data are extracted from
 235 the Seismological Instrumental and parametric Data-base (ISIDe) website (last accessed 22/07/15).

#	Date and Time (UTC)	Latitude [°]	Longitude [°]	Depth [km]	Magnitude	
1	06/04/09 01:32	42.342	13.38	8.3	6.1	M_w
2	06/04/09 01:36	42.352	13.346	9.7	4.7	M_L
3	06/04/09 02:37	42.360	13.328	8.7	4.8	M_w
4	06/04/09 23:15	42.463	13.385	9.7	5.0	M_w
5	07/04/09 09:26	42.336	13.387	9.6	4.9	M_w
6	07/04/09 17:47	42.303	13.486	17.1	5.4	M_w
7	09/04/09 00:53	42.489	13.351	11.0	5.2	M_w
8	09/04/09 19:38	42.504	13.350	9.3	5.0	M_w
9	13/04/09 21:14	42.498	13.377	9.0	4.8	M_w

236

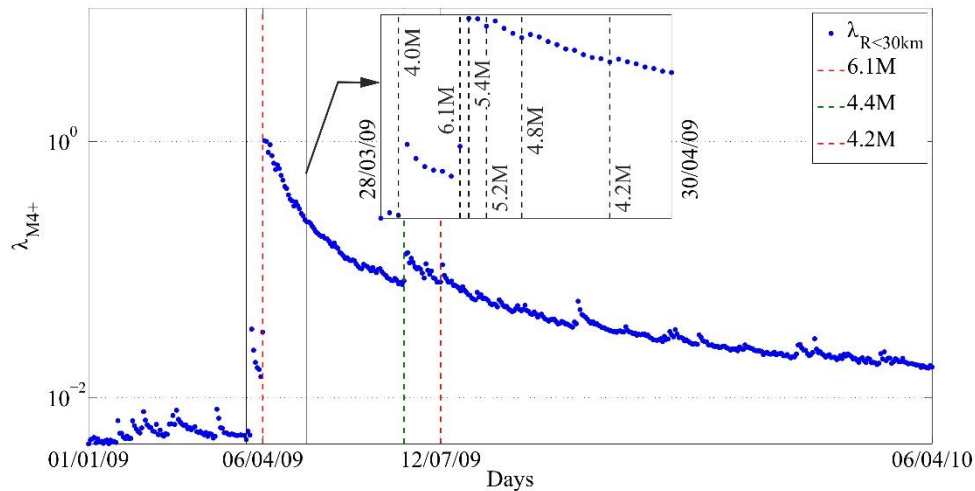
[§] It is to note that, the epicentre location of the mainshock of the sequence is known only afterwards. Conversely, in using MANTIS-K during a seismic sequence, some hypotheses on the location of the geographic area to be monitored would be required.

237 The geographic area affected by the sequence is reported in Figure 4a and Figure 4b; both of them show
 238 boundaries of municipalities and the mainshock epicentre (represented by a star). Figure 4a displays the grid
 239 of point-like seismic sources, the OEF-Italy system assigns earthquake rates to. Figure 4b reports the centroids
 240 of each municipality for which loss indices are computed together with contours of the distance from the
 241 epicentre of the mainshock, R .



242
 243 Figure 4. Geographic representation of the mainshock epicentre together with (a) the grid of the point-like seismic sources
 244 according to OEF-Italy and (b) the centroids of municipalities within 70 km from the epicentre.

245 In order to provide a synthetic representation of the forecasted seismicity during the whole sequence, the values
 246 of seismic rates provided by OEF-Italy, for each point-like source within 30 km from the epicentre of the
 247 mainshock (see Figure 4a), are summed up and plotted in Figure 5 as a function of the day in which rates were
 248 have been released by the INGV system. In the same figure, the dates of occurrence of all $M_W 4.2+$ events are
 249 also reported with dotted vertical lines. It is to note that the event rates during the seismic crisis are two orders
 250 of magnitude larger than those computed at the beginning of 2009. It is also to underline that the maximum is
 251 on the day after the mainshock of the sequence; this is a feature of the OEF-Italy system according to which
 252 the rates peak right after the maximum seismic moment release (Marzocchi and Lombardi, 2009). Similarly, a
 253 significant increment of forecasted rates can be identified after all the *strong* events of the sequence. In fact,
 254 although discussion of pro and cons of OEF is out of the scope of this paper, it has to be anticipated that trend
 255 of the seismic loss estimates from the MANTIS-K system reflect the trend in time of OEF-Italy rates.



256

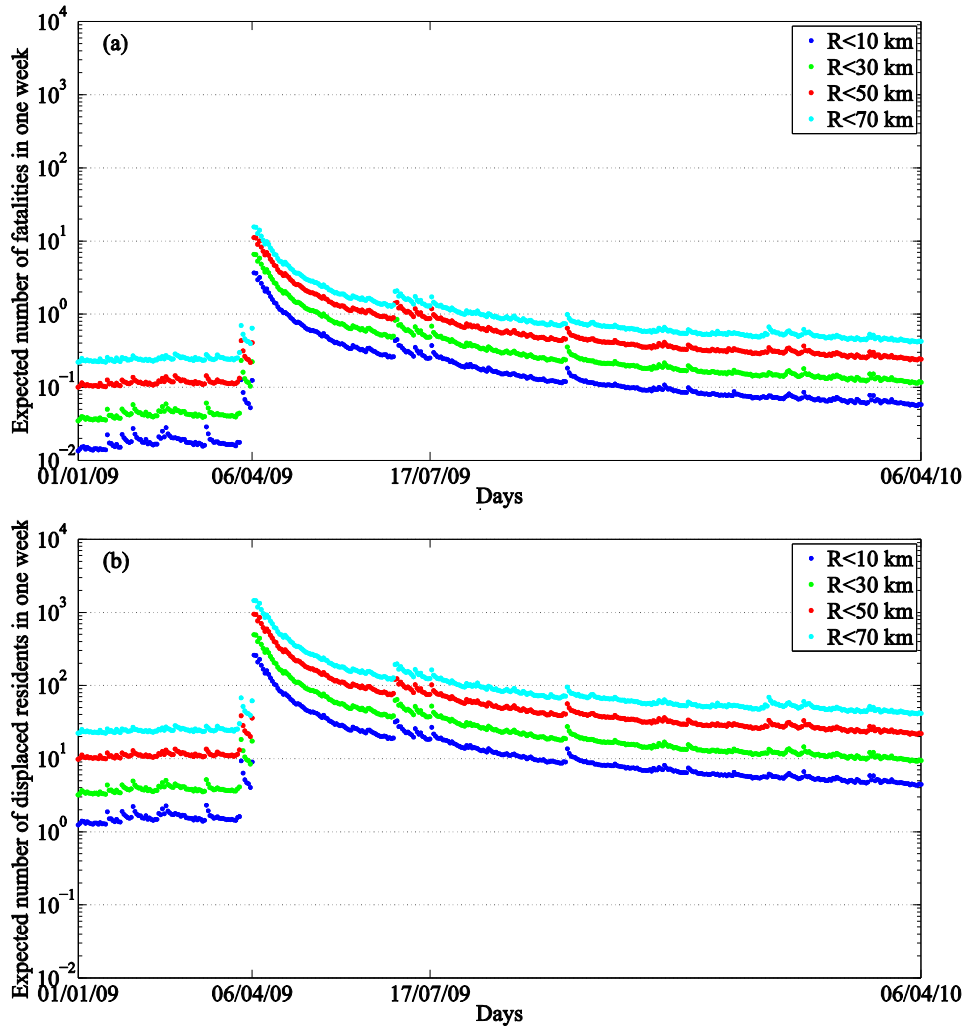
257 Figure 5. Sum of the following week's (with respect to the date in the abscissa) rates of M 4+ events within 30 km from
 258 the centre of the sequence, and dates of M 4.2+ events occurred in the area of Figure 1 (see also Table 1 for date of each
 259 event). In the picture, M refers to moment magnitude M_w .

260 Figure 6a shows the evolution of the expected number of total fatalities, for municipalities within 10 km, 30
 261 km, 50 km and 70 km from the epicentre of the mainshock (see Figure 4 for the identification of such
 262 municipalities).

263 At the beginning of 2009 the expected value of fatalities in one week is lower than one for the whole area
 264 considered around the centre of the sequence (i.e., about 0.22 for $R < 70$ km on 01/01/2009). Five days before
 265 the mainshock, the trend of loss shows some increments (due to the M_w 4.0 event on the 30th of March) and
 266 the expected fatalities for the week after 06/04/09 are about 0.64 within 70 km. Results change right after the
 267 mainshock when the expected number of total fatalities becomes larger than one; i.e., 3.7, 6.5, 11.1 and 15.5
 268 for radii of 10 km, 30 km, 50 km and 70 km, respectively. ** One year after the mainshock, the maximum value
 269 of the expected number of fatalities is around 0.4 that is comparable with the reported value computed at the
 270 beginning of 2009; i.e., the sequence seems have come to an end.

271 Figure 6b shows the expected number of total displaced residents. The maximum value is equal to 1452.5
 272 within 70 km from the epicentre of the mainshock (940.1, 493.4 and 259.8 for radii in descending order).

** Note that after a damaging earthquake, evacuation is likely to be expected, while at this stage the algorithm of MANTIS-K assumes stable exposure (and also vulnerability), despite the occurred earthquake.



273

274 Figure 6. Expected number of (a) fatalities and (b) displaced residents in the week following the date in the abscissa,
 275 summed over all municipalities within 10 km, 30 km, 50 km and 70 km from the centre of the sequence.

276 3.2 Emilia 2012

277 The prominent magnitude event of the sequence, the mainshock, is the M_w 5.8 occurred on the 20th of May
 278 2012 (see also Iervolino et al., 2012). The aftershock sequence, until the end of May 2013, and in the box
 279 identified by 44.5-45.5 °N latitude and 10.5-12.0 °E longitude (see also Figure 1), includes 13 M 4.5+ events
 280 reported in Table 2 (data from ISIDE, last accessed 20/07/15). The (*first*) mainshock and the M_w 5.6 event on
 281 the 29th of May (sometimes referred to as *second* mainshock; e.g., Dolce and Di Bucci, 2015) were felt in the
 282 whole Northern Italy. (Dates in Table 2 show a difference with respect to the case of L'Aquila. Indeed, most

283 of the largest magnitude events occurred few hours after the two mainshocks.) The recorded largest (corrected)
 284 horizontal PGAs are about 259 cm/s² and 495 cm/s² for the 5.8 and 5.6 M_w event, respectively.††

285 Following the first strong event, on the 22nd of May, the Italian government declared the emergency for
 286 the provinces of Modena, Ferrara, Bologna and Mantova. On the 30th of May, after the M_w 5.6 event, the state
 287 of emergency was extended to the provinces of Reggio Emilia and Rovigo.

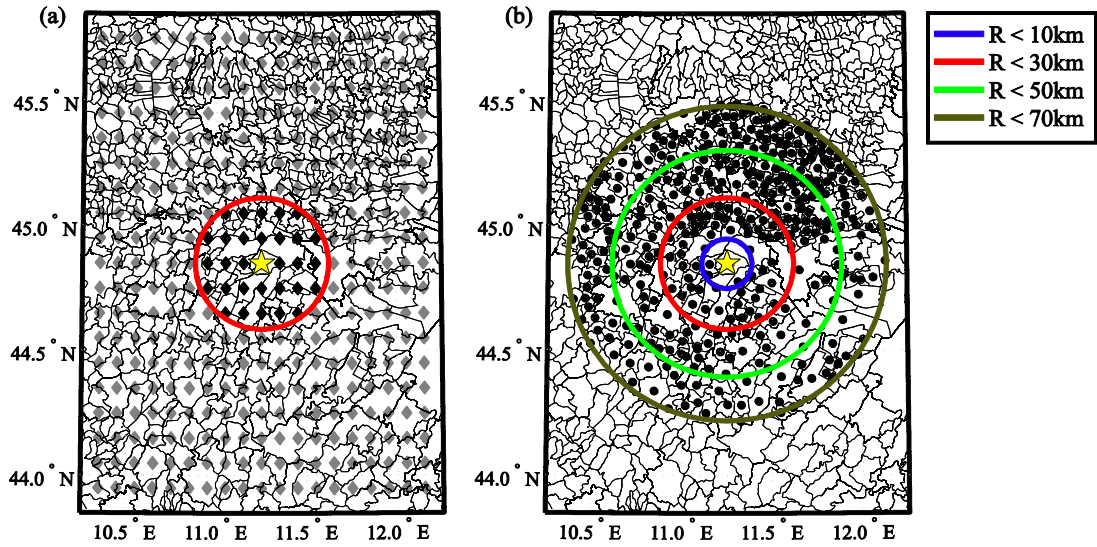
288 Table 2. M 4.5+ earthquake in a geographic area within latitude 44.5°-45.5° and longitude 10.5°-12.0°. Reported
 289 information are event date and time, hypocentre latitude, longitude and depth, event magnitude. Data are extracted from
 290 ISIDe website (last accessed 20/07/15).

#	Date and Time (UTC)	Latitude [°]	Longitude [°]	Depth [km]	Magnitude	
1	20/05/12 02:03	44.896	11.264	9.5	5.8	M_w
2	20/05/12 02:06	44.879	11.120	5.0	4.8	M _L
3	20/05/12 02:06	44.905	11.165	4.3	4.8	M _L
4	20/05/12 02:07	44.874	11.270	6.1	5.0	M _L
5	20/05/12 03:02	44.860	11.152	9.1	5.0	M _L
6	20/05/12 13:18	44.814	11.441	3.4	4.9	M _w
7	20/05/12 17:38	44.880	11.253	3.7	4.6	M _L
8	29/05/12 07:00	44.842	11.066	8.1	5.6	M_w
9	29/05/12 08:25	44.865	10.948	7.9	5.0	M _L
10	29/05/12 08:27	44.883	11.042	6.0	4.6	M _L
11	29/05/12 10:55	44.865	10.980	4.4	5.3	M _w
12	29/05/12 11:00	44.856	10.941	8.7	5.0	M _L
13	29/05/12 11:00	44.866	10.976	7.2	5.1	M _L
14	03/06/12 19:20	44.886	10.950	8.7	4.7	M _w

291 Similarly to L'Aquila, Figure 7a shows the point-like seismic sources in the area of interest, identifying those
 292 within 30 km from the epicentre of the mainshock; Figure 7b displays the centroids of municipalities within
 293 the four boundaries presented results refer to; i.e., radii lower than 10 km, 30 km, 50 km and 70 km.

295 The distribution in time of the main aftershocks, clustered in the few days after the mainshock, is
 296 reflected by the evolution of forecasted seismic rates (Figure 8) that has a regular trend decreasing with the
 297 increasing time after the M_w 5.6 event. It is to note that maximum forecasted seismicity corresponds to the day
 298 after the second mainshock that has, in fact, a magnitude lower than the first one.

†† The values of PGA are available on the Italian Accelerometric Archive – ITACA - <http://itaca.mi.ingv.it/>, last accessed 20/07/15. However, note that for the second event ITACA does not specifies whether the PGA has been recorded in free field conditions. In fact, Dolce and Di Bucci (2015) report a maximum horizontal PGA value for the second event of 289 cm/s².

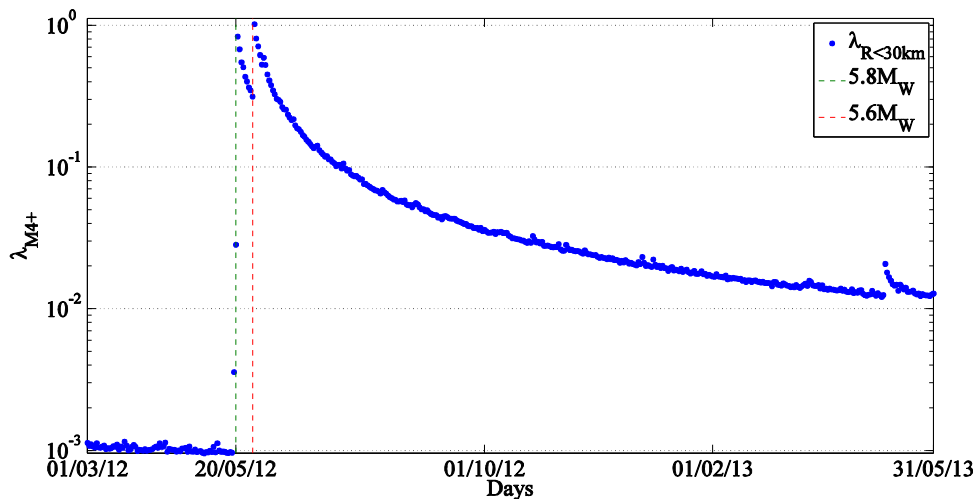


299

300 Figure 7. Geographic representation of the mainshock epicentre together with (a) the grid of the point-like seismic sources
 301 according to OEF-Italy and (b) the centroids of municipalities within 70 km from the epicentre.

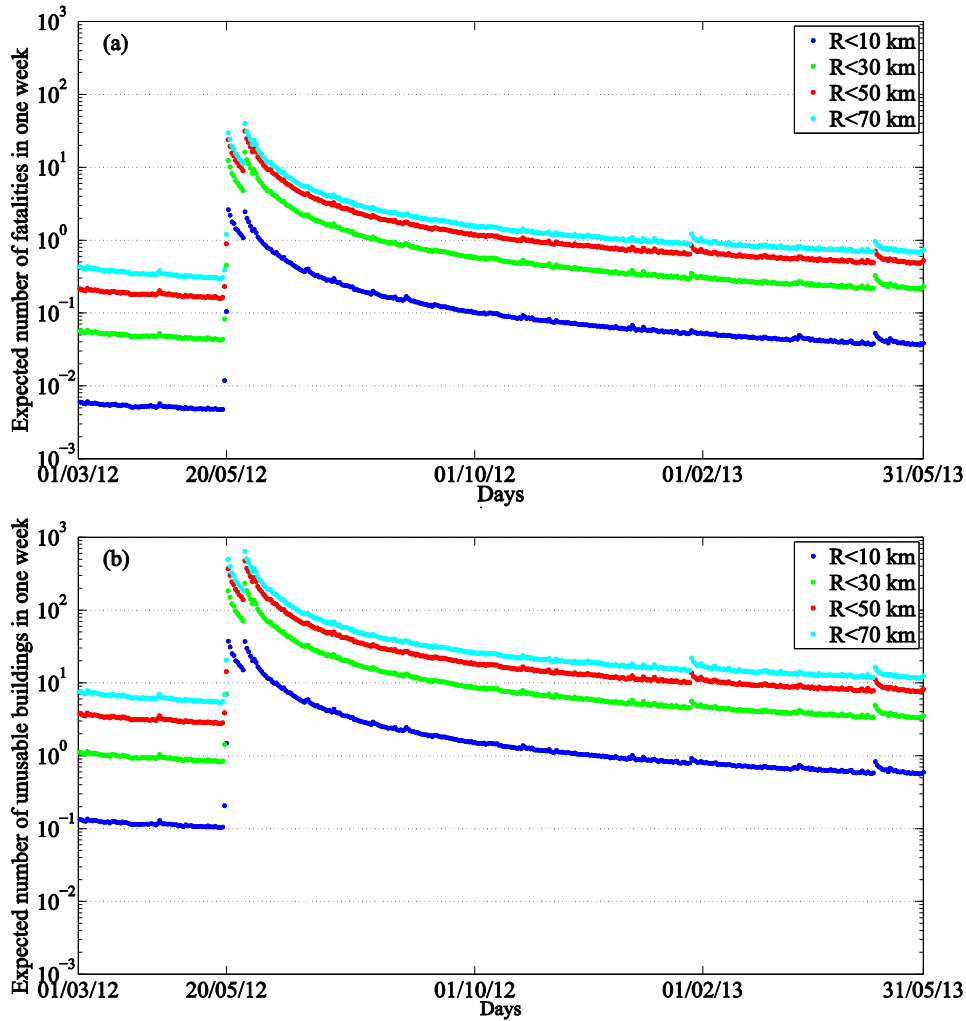
302 Figure 9 shows the expected values of fatalities and unusable buildings in the time interval of Figure 8.

303 Expected number of fatalities for the week after 00:00 of 20/05/12 (i.e., right before the mainshock) are 0.1,
 304 0.5, 0.9 and 1.2 for the municipalities within radii of 10 km, 30 km, 50 km and 70 km from the centre,
 305 respectively. The same estimates right after the mainshock (i.e., for the week after 21/05/12) become 2.6, 12.3,
 306 23.8 and 29.7, respectively. For the week after 29/05/12, values are about 1.1, 4.8, 8.9 and 11.1 and become
 307 2.5, 16.0, 31.2 and 39.5, after the M_w 5.6. In the same period, the largest numbers of expected unusable
 308 buildings are 36.9, 232.9, 471.9 and 639.0.



309

310 Figure 8. Sum of the following week's (with respect to the date in the abscissa) rates of M 4+ events within 30 km from
 311 the centre of the sequence, and dates of main events occurred in the area.



312

313 Figure 9. Expected number of (a) fatalities and (b) unusable buildings in the week following the date in the abscissa,
 314 summed over all municipalities within 10 km, 30 km, 50 km and 70 km from the centre of the sequence.

315 3.3 Garfagnana 2013

316 The mainshock of this sequence was the M_w 5.1 on the 21st of June 2013 and, consistent with previous cases,
 317 the considered time window extends to about one year after this date. However, on the 25th of January 2013, a
 318 M_w 4.8 struck in the same area (identified in Figure 1; 43.5-44.5 °N and 9.5-11.0 °E). Thus, available data
 319 were analysed starting from about three months before this event; i.e., from the 1st of November 2012.

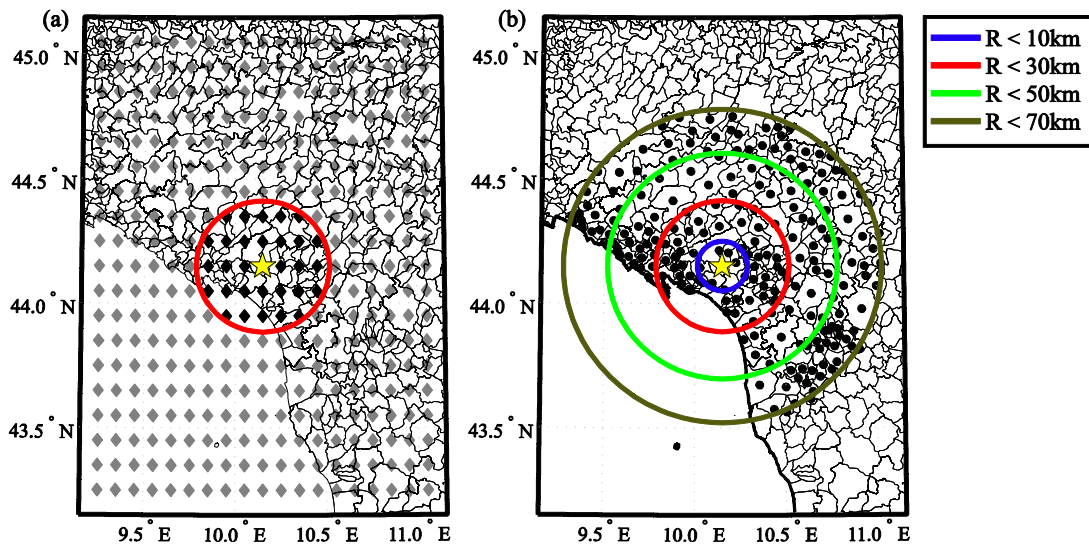
320 From November 2011 to the mainshock, 20 M 2.5+ earthquakes stoke in the area; among these events, 6
 321 had magnitude equal to or larger than 3.0, and 1 larger than 4.0 (the one of M_w 4.8). In the 24 hours after the
 322 mainshock, 12 earthquakes occurred in the area, all with magnitude between 3 and 4. The subsequent event
 323 with M equal to 4.5 occurred on the 30th of June 2013. Table 3 shows the 5 events with M equal to or larger
 324 than 4 in the considered area and time interval.

325 During the sequence, someone claimed similarities with respect to seismic events preceding L'Aquila
 326 mainshock (authors are not aware of scientific studies supporting such a similarity). In fact, the sequence
 327 focalised the attention of mass media and the worries of residents, and the Italian civil protection department
 328 was constantly in state of attention.**

329 Table 3. M 4.0+ earthquake in a geographic area within latitude 43.5°-44.5° and longitude 9.5°-11.0°. Reported
 330 information are event date and time, hypocentre latitude, longitude and depth, event magnitude. Data are extracted from
 331 ISIDE website (last accessed 20/07/15).

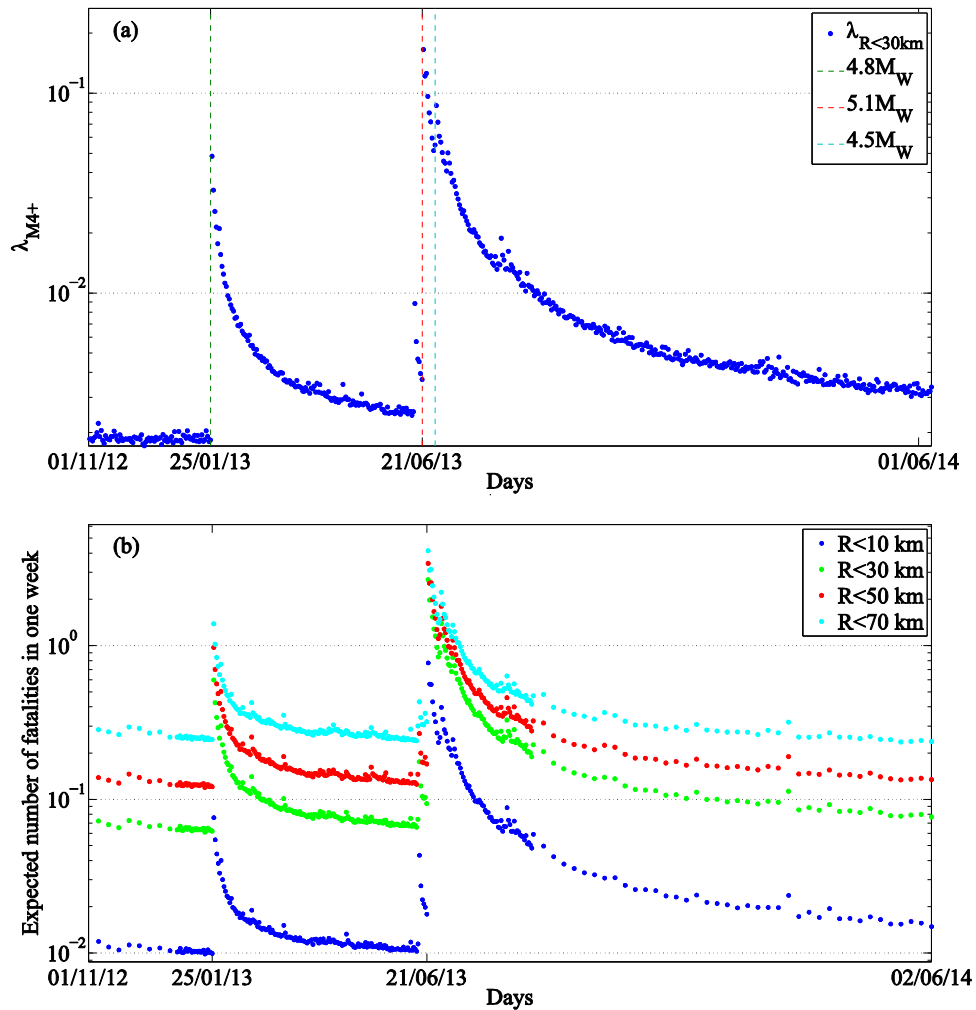
#	Date and Time (UTC)	Latitude [°]	Longitude [°]	Depth [km]	Magnitude	
1	25/01/13 14:48	44.164	10.446	19.80	4.8	M _w
<u>2</u>	<u>21/06/13 10:33</u>	<u>44.090</u>	<u>10.062</u>	<u>5.70</u>	<u>5.1</u>	<u>M_w</u>
3	21/06/13 12:12	44.162	10.135	8.10	4.0	M _w
4	23/06/13 15:01	44.168	10.201	9.20	4.4	M _w
5	30/06/13 14:40	44.160	10.187	6.10	4.5	M _w

332
 333 The point-like seismic sources within 30 km from the epicentre of the mainshock are reported in Figure 10a
 334 while centroids of municipalities and boundaries of interest for results are shown in Figure 10b. The evolution
 335 of the sum OEF rates within 30 km from the epicentre of the mainshock is clearly affected by the two largest
 336 magnitude events as reported in Figure 11a.



337
 338 Figure 10. Geographic representation of the mainshock epicentre together with (a) the grid of the point-like seismic
 339 sources according to OEF-Italy and (b) the centroids of municipalities within 70 km from the epicentre.

** See <http://terremoti.ingv.it/it/ultimi-eventi/921-evento-sismico-tra-le-province-di-lucca-e-massa.html>, last accessed 20/07/15.



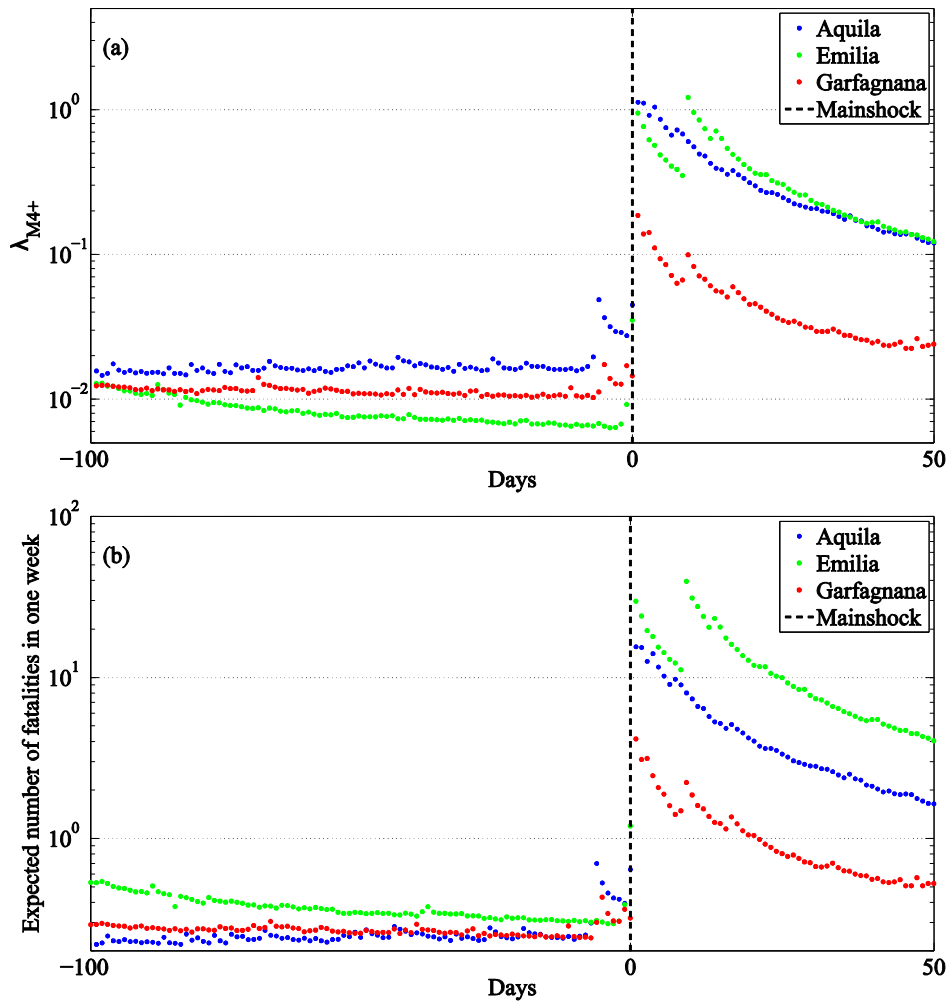
340 Figure 11. (a) Sum of the following week's (with respect to the date in the abscissa) rates of M 4+ events within 30 km
 341 from the centre of the sequence, and dates of main events occurred in the area; (b) weekly expected number of fatalities
 342 summed over all municipalities within 10 km, 30 km, 50 km and 70 km from the centre of the sequence.
 343

344 Expected values of fatalities are reported in Figure 11b. For the week after 25th of January 2013, loss estimates
 345 are lower than one (0.2 within 70 km from the centre of the sequence). For the week after 26/01/13, the same
 346 estimation becomes about 1.4 and decreases in the subsequent days with a regular path. A peculiar trend can
 347 be identified in the six days before the mainshock: about 0.3 is the expected number of fatalities within 70 km
 348 for the week after 21/06/13 (i.e., right before the mainshock), and it becomes 4.1 for the week after the day of
 349 the mainshock.

350 3.4 Sequences' comparison

351 Figure 12 shows, for the three analysed sequences, (a) the sum of the weekly rates of M 4+ events within 70
 352 km from the centre of the shock and (b) the weekly expected fatalities in the same areas. In the figure, for the

353 sake of comparison, the days of the mainshocks are coincident and the chosen time window goes from 100
 354 days before to 50 days after the mainshock.



355
 356 Figure 12. (a) Sum of the following week's (with respect to the time in the abscissa) rates of M 4+ events within 70 km
 357 from the centre of each sequence; (b) weekly expected number of fatalities within 70 km from the centre of each sequence.
 358 The comparison between Figure 12a and Figure 12b underlines, once again, that the results of MANTIS-K are
 359 more informative than those of OEF, because it accounts not only for hazard but also for vulnerability and
 360 exposure. Indeed, in the whole considered time-window before the mainshock, seismic rates for L'Aquila are
 361 larger than those for Garfagnana and Emilia (in this latter case the rates are the lowest). Conversely, the
 362 expected fatalities for L'Aquila and Garfagnana are comparable, while the largest are associated to the Emilia
 363 sequence.^{§§} Similarly, after the mainshock, the seismicity rates for L'Aquila and Emilia are comparable, and
 364 both higher than Garfagnana. On the other hand, the expected losses for Emilia are significantly higher than

^{§§} See Dolce and Di Bucci (2015) for a discussion, related to exposure, which may help in understanding this result.

365 those expected in L'Aquila, and the expected losses in Garfagnana are lower than those of the other sequences.
366 Considering only the seven days before the mainshock, it is also interesting to note that L'Aquila shows some
367 increment of expected losses with respect to previous weeks, while the Emilia shows significant expected loss
368 variations only since the day before the mainshock, Figure 12b. This trend can be also identified in terms of
369 seismic rates (Figure 12a).

370 **3.5 Observed losses and the meaning of OELF results**

371 In this section the consequences observed in the analysed earthquakes are reported (see Dolce and Di Bucci,
372 2015, for details). Indeed, it is believed appropriate to discuss the losses produced in the seismic sequences to
373 better understand the intrinsic meaning of OELF and the current features and/or limitations of MANTIS-K.

374 For what concerns L'Aquila, 308 total fatalities have been counted. Approximately 34000 buildings failed
375 or resulted unusable, at least 1500 residents were injured and more than 65000 were temporarily displaced.
376 During the Emilia sequence the number of dwelling buildings declared unusable after a survey was in the order
377 of 15000. Fatalities reported are 26, 7 of which are due to the mainshock on the 20th of May, and 19 to the
378 second event on the 29th of May. Finally, in the Garfagnana sequence, no significant damage or injuries have
379 been observed.

380 Even if OELF provides losses' predictions, there is a number of reasons why direct comparison of the
381 observed consequences with the results of OELF, if not inappropriate, requires at least particular caution. First
382 of all, OELF provides weekly expected values. In statistical terms, the expected value is the limit of the
383 arithmetic mean over a virtually infinite number of nominally equivalent trials. In this respect, the observed
384 losses are individual realizations only, which do not allow validation (see also Iervolino, 2013, for a discussion
385 of similar issues). It is also to note that OELF, by nature of the OEF models providing the input rates, provides
386 the largest expected losses only after the strongest event of the sequence, while a significant portion of the
387 consequences observed is due to the main events (e.g., in the L'Aquila case).

388 In addition to this basic discussion of the meaning of OELF, it has to be recalled that at this stage there
389 are some features/limitations of MANTIS-K, which are relevant to the analysis of the observed losses. For
390 example, most of the fatalities occurred during the Emilia sequence were in industrial buildings and not in
391 residential buildings, which are those at the basis of damage vulnerability matrices and exposure data.

392 Moreover, it is to also underline that MANTIS-K does not account for damage accumulation. Although it is
393 something feasible to consider, it is not yet implemented, while it may be relevant to sequences with multiple
394 potentially-damaging events, such as the Emilia one. In these cases, the vulnerability of the building stock
395 varies during the sequence (e.g., Iervolino et al., 2014b and 2015b). Finally, also exposure may significantly
396 vary, affecting the losses, in a sequence featuring at least one damaging event due to precautionary evacuations;
397 e.g., L'Aquila. Also this issue could be accounted for in the MANTIS-K approach, yet it is something not yet
398 in place.

399 **4. Conclusions**

400 The study focused on a retrospective analysis of three Italian seismic sequences through the recently developed
401 MANTIS-K system for short-term earthquake loss forecasting. Indeed, seismicity rates estimated by the OEF-
402 Italy system are the input data for MANTIS-K that, performing a probabilistic analysis, is able to convert them
403 into weekly estimates of seismic losses (e.g., expected values of fatalities, displaced residents, and damaged
404 buildings), using vulnerability and exposure data and models at the municipality scale for Italy.

405 The seismic sequences, chosen for the critical analysis of OELF, are L'Aquila (2009), Emilia (2012) and
406 Garfagnana (2013), which include the main earthquakes occurred in Italy from 2004 to 2014. For each of the
407 sequences, risk measures for areas characterised by different values of radius from the mainshock epicentre
408 (10 km, 30 km, 50 km and 70 km) were considered. It was observed that the trends of forecasted losses are, as
409 expected, strongly influenced by OEF input data. In particular, due to the features of the OEF-Italy system, the
410 largest increment of the expected losses are always right after the maximum seismic moment release (i.e., for
411 the week after the largest events in the sequence).

412 A discussion of the observed losses in the sequences allowed to discuss the meaning of the OELF
413 predictions as well as the current features and/or limitations of the MANTIS-K system. In fact, the statistical
414 interpretations of the expected loss was recalled. Moreover, the cases of the L'Aquila and the Emilia sequences
415 allowed to point out that during seismic sequence with one or more damaging events, damage accumulation
416 in the building stock and precautionary evacuations, may lead to short-term variations of vulnerability and
417 exposure that may affect the expected losses, yet are not accounted for at this stage. Finally, MANTIS-K relies

418 on dwelling building exposure, not suitable to reflect peculiar structural typologies, which may also affect the
419 losses, as observed, for example, with precast industrial buildings in the Emilia sequence.

420 Even with the discussed issues and limitations, it is believed that OELF implemented in the MANTIS-K
421 system is a step in the direction of rational decision making for risk management during seismic sequences
422 due to its quantitative approach, and it is certainly more informative than OEF alone.

423 **5. Acknowledgments**

424 The study presented in this paper was developed in the framework of *AMRA – Analisi e Monitoraggio dei Rischi*
425 *Ambientali scarl* (<http://www.amracenter.com>) for the *strategies and tools for real-time earthquake risk reduction*
426 (REAKT; <http://www.reaktproject.eu>) funded by the European Commission via the *Seventh Framework Program for*
427 *Research*, with contract no. 282862. Professor Mauro Dolce and Dr. Warner Marzocchi are gratefully acknowledged for
428 their comments, which improved quality and readability of this paper.

429 **6. References**

- 430 Braga F, Dolce M, Liberatore D (1982) Southern Italy November 23 1980 Earthquake: A Statistical Study on Damaged
431 Buildings and an Ensuing Review of the M.S.K.-76 Scale. Proc. of 7th European conference on earthquake
432 engineering, ECEE, CNR-PFG n.503, Rome, Italy.
- 433 Chioccarelli E, De Luca F, Iervolino I (2009) Preliminary study of L'Aquila earthquake ground motion records V5. 20.
434 ReLUIS Report, available at: http://www.reluis.it/doc/pdf/Aquila/Peak_Parameters_L_Aquila_Mainshock_V5.2.pdf
- 435 Cornell CA, Krawinkler H (2000) Progress and challenges in seismic performance assessment. PEER Center News 3:1-
436 3.
- 437 Dolce M, Di Bucci D (2015) Comparing recent Italian earthquakes. Bull Earthq Eng. DOI 10.1007/s10518-015-9773-7.
438 (in press)
- 439 Gerstenberger M, Wiemer S, Jones LM, Reasenberg PA (2005) Real-time forecasts of tomorrow's earthquakes in
440 California. Nature 435: 328 – 331.
- 441 Gutenberg B, Richter CF (1944) Frequency of earthquakes in California. Bull Seismol Soc Am 34:185-188.
- 442 Iervolino I (2013) Probabilities and Fallacies: Why Hazard Maps Cannot Be Validated by Individual Earthquakes. Earthq
443 Spectra, 29:1125-1136.
- 444 Iervolino I, Chioccarelli E, Giorgio M, Marzocchi W, Lombardi AM, Zuccaro G, Cacace F (2014a) Operational
445 earthquake loss forecasting in Italy: preliminary results. Proc. of Second European Conference on Earthquake
446 Engineering and Seismology, Istanbul, Turkey.

447 Iervolino I, Chioccarelli E, Giorgio M, Marzocchi W, Zuccaro G, Dolce M, Manfredi G (2015a) Operational (short-term)
448 earthquake loss forecasting in Italy. *Bull Seism Soc Am* 105:2286–2298.

449 Iervolino I, De Luca F, Chioccarelli E (2012) Engineering seismic demand in the 2012 Emilia sequence: preliminary
450 analysis and model compatibility assessment. *Ann Geophys-Italy* 55:639-645.

451 Iervolino I, Giorgio M, Polidoro B (2015b) Reliability of structures to earthquake clusters. *Bull Earthq Eng*, 13:983–
452 1002.

453 Iervolino I, Giorgio M, Chioccarelli E (2014b) Closed-form aftershock reliability of damage-cumulating elastic-perfectly-
454 plastic systems. *Earthq Eng Struct D* 43:613–625.

455 Jordan TH, Chen Y-T, Madariaga R, Main I, Marzocchi W, Papadopoulos G, Sobolev G, Yamaoka K, Zschau J. (2011)
456 Operational earthquake forecasting – State of the knowledge and guidelines for utilization. *Ann Geophys-Italy*
457 54:319-391.

458 Marzocchi W, Iervolino I, Giorgio M, Falcone G. (2015) When is the probability of a large earthquake too small? *Seism*
459 *Res Lett*. DOI 10.1785/0220150129 (In press)

460 Marzocchi W, Lombardi AM (2009) Real-time forecasting following damaging earthquake. *Geop Res Lett* 36: L21302.

461 Marzocchi W, Lombardi AM, Casarotti E (2014) The establishment of an operational earthquake forecasting system in
462 Italy. *Seismol Res Lett* 85:961-969.

463 McGuire RK (2004) Seismic hazard and risk Analysis. Earthquake Engineering Research Institute Publication, Oakland,
464 California, Monograph MNO-10.

465 Ogata Y (1988) Statistical models for earthquake occurrences and residual analysis for point processes. *J Am Stat Ass*
466 83:9-27.

467 Ogata Y (1998) Space-time point-process models for earthquake occurrences. *Ann Inst Stat Math* 50:379-402.

468 Pasolini C, Albarello D, Gasperini P, D'Amico V, Lolli B (2008) The attenuation of seismic intensity in Italy, Part II:
469 Modelling and Validation. *Bull Seismol Soc Am* 98:692-708.

470 Sieberg A (1931) Erbeben, in *Handbuch der Geophysik*. B. Gutenberg (Editor) 4:552–554. (In German).

471 Zuccaro G, Cacace F (2011) Seismic casualty evaluation: the Italian model, an application to the L'Aquila 2009 event. In
472 *Human Casualties in Earthquakes: progress in modelling and mitigation*, R. Spence, E. So, and C. Scawthorn
473 (Editors), Springer, London, UK.

474 Zuccaro G, Cacace F, De Gregorio D (2012) Buildings inventory for seismic vulnerability assessment on the basis of
475 Census data at national and regional scale. *Proc. of 15th World Conference on Earthquake Engineering*, Lisbon,
476 Portugal.

477 Zuccaro G, Cacace F (2009) Revisione dell'inventario a scala nazionale delle classi tipologiche di vulnerabilità ed
478 aggiornamento delle mappe nazionali di rischio sismico. *Proc. of XIII Convegno l'Ingegneria Sismica in Italia*,
479 ANIDIS, Bologna, Italy. (In Italian)

480 Whitman RV, Reed JW, Hong ST (1973) Earthquake Damage Probability Matrices. *Proc. of 5th World Conference on*
481 *Earthquake Engineering*, WCEE, Rome, Italy.